COLLOQUIA: La Thuile 2016

Heavy vector resonances at the LHC

A. THAMM

PRISMA Cluster of Excellence & Mainz Institute for Theoretical Physics, Johannes Gutenberg University - Mainz, Germany

Summary. — This contribution discusses a model-independent approach to study heavy vector triplets at the LHC. The simplified model parameterizes single production and decay of the heavy vectors. Specific, weakly and strongly coupled models can be easily matched to the simplified Lagrangian. Thus, if experimental results are presented in terms of these simplified model parameters, the interpretation of experimental limits in a wide range of explicit models is straightforward. Finite width effects have to be accounted for in order to set reliably model-independent bounds.

1. – Introduction and summary

Searches for heavy vector particles are theoretically well motivated since their existence is predicted by many extensions of the Standard Model (SM). In order to obtain as much information as possible about such new particles, couplings to quarks, leptons, SM gauge bosons and Higgses have to be investigated. All of these couplings are present, and in principle sizeable, for a colourless electroweak triplet heavy vector with zero hypercharge and we thus choose this as a motivated representative to study. Many experimental searches at 8 and 13 TeV have already been performed by ATLAS and CMS. A particularly useful and broadly applicable approach would be to present the experimental limits not only in terms of cross-section times branching ratio but also in terms of simplified model parameters which describe the relevant LHC phenomenology of a heavy triplet. Specific models with a heavy triplet can easily be matched to the simplified Lagrangian and thus bounds on specific model parameters can be inferred. The simplified Lagrangian thus builds a bridge between the experimental limits and a variety of explicit theoretical models.

To ensure that experimental limits are set on cross-section times branching ratio, a model-independent quantity, finite width effects have to be minimised. Two well-known effects are distortions of the Breit-Wigner distribution due to rapidly decreasing parton luminosities and due to quantum mechanical interference with the background. Both

effects are discussed in more detail in sect. **3** and can be kept under control by focussing on the peak region of the invariant mass distribution. Thus, considering only a narrow window around the peak allows us to set model-independent experimental bounds which can be expressed in terms of simplified model parameters and interpreted within a large range of explicit models.

This approach has been discussed in detail for an electroweak triplet in ref. [1] but could also be useful for further representations. Other representations include colourless electroweak singlets with zero or unit hypercharge [2] and an electroweak doublet and triplet with hypercharge $-3/2$ and 1 respectively. Note that in the latter two cases couplings to quarks and fermions, respectively, are lacking, which reduces their importance at the LHC significantly.

2. – Heavy vector triplets

A heavy vector triplet consists of two essentially degenerate states: an electrically charged, $V^\pm$, and a neutral one, V^0. The Lagrangian is given as

$$
\begin{aligned}
\mathcal{L}_V \;=\; & -\frac{1}{4} D_{[\mu} V^a_{\nu]} D^{[\mu} V^{\nu] \, a} + \frac{m_V^2}{2} V^a_\mu V^{\mu \, a} \\
& + i\, g_V c_H V^a_\mu H^\dagger \tau^a \overleftrightarrow{D}{}^\mu H + \frac{g^2}{g_V} c_F V^a_\mu J^{\mu \, a}_F \\
& + \frac{g_V}{2} c_{VVV}\, \epsilon_{abc} V^a_\mu V^b_\nu D^{[\mu} V^{\nu] \, c} + g_V^2 c_{VVHH} V^a_\mu V^{\mu \, a} H^\dagger H \\
& - \frac{g^2}{2} c_{VVW} \epsilon_{abc} W^{\mu \nu \, a} V^b_\mu V^c_\nu \,.
\end{aligned}
\tag{1}
$$

The couplings of the triplet to all SM particles are given in terms of the new coupling g_V, which parameterizes the interaction strength between the heavy vectors. The relevant parameter space of a triplet with a given mass is two-dimensional consisting of two parameter combinations which describe its couplings to fermions and to SM gauge bosons, as shown in the second line of eq. (1). All interactions in the third and fourth line of the Lagrangian (1) involve two or more heavy vector fields. They are neither relevant for single production of the heavy vectors nor for their decay and have thus a negligible effect on the LHC phenomenology of the triplet.

This setup is extremely versatile since it can capture the features of many, weakly and strongly coupled, concrete models. For illustration, two explicit models are chosen as benchmarks. First, an extended gauge symmetry discussed in ref. [3] can be used as an example of a weakly coupled model, referred to as model A in the following. Values of the coupling g_V are of order one in these models. Second, we consider the strongly interacting Minimal Composite Higgs Model [4], referred to as model B, which is valid for larger values of g_V. Values within the range $1 \lesssim g_V \lesssim 4\pi$ are acceptable. Since the width of the heavy vector triplet, Γ, grows with g_V in model B, large values of g_V do not produce a narrow resonance. In order to focus on narrow resonances we consider values of g_V within the range $1 \lesssim g_V \lesssim 6$ for which Γ/m_V never exceeds around 10%.

The coupling of V to fermions scales as $g^2/g_V c_F$, where g is the SM $SU(2)_L$ gauge coupling and c_F is a free parameter which can be fixed in an explicit model. In both benchmark models A and B, c_F is expected to be of order one. The coupling to fermions in strongly interacting models is thus suppressed by g/g_V with respect to weakly coupled models. Thus, in general, a large coupling g_V corresponds to a small Drell-Yan production rate and, similarly, a small branching ratio into fermionic final states. The heavy vector
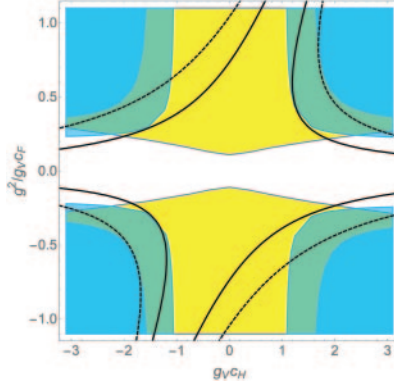
Fig. 1. – Contours of experimental searches for a 2 TeV resonance in the parameter space $(g_V c_H, g^2/g_V c_F)$. The yellow region shows the exclusion from the CMS search in the $l\nu$ final state at 8 TeV [5] and the very close lying dashed yellow line depicts the $l\nu$ search at 13 TeV [6]. The dark blue region is excluded by the di-boson searches into two fat jets at 8 TeV [7] while the light blue region represents the exclusion from the 13 TeV CMS search into a fully hadronic and semi-leptonic final state [8]. The black lines represent bounds from electroweak precision tests. CMS searches have been used for illustration, however the corresponding ATLAS searches lead to the same conclusions.

triplet couples dominantly to the longitudinal components of the gauge bosons and to the Higgs through the term proportional to c_H, while the coupling to transverse gauge bosons is generally suppressed since the corresponding terms originate from the mixing between V and the SM W boson. Note that this Lagrangian predicts the same branching ratio for the four processes

$$(2) \quad \mathrm{BR}(V^\pm \to W^\pm Z) = \mathrm{BR}(V^\pm \to W^\pm h) = \mathrm{BR}(V^0 \to W^\pm W^\pm) = \mathrm{BR}(V^0 \to Zh).$$

Contrary to the coupling to fermions, the V coupling to SM bosons scales as $g_V c_H$. The parameter c_H, analogously to c_F, has to be fixed in each concrete model and takes values of order one in models A and B. Here we have the reversed situation: a small value of g_V in weakly coupled extensions of the SM leads to a small branching fraction into gauge bosons, while strongly coupled theories predict an enhanced branching ratio. Thus strongly and weakly interacting heavy vectors are expected to have a very different phenomenology: weakly coupled vectors are produced copiously through Drell-Yan, decay predominantly into two leptons or jets and have a small branching ratio into gauge bosons; strongly interacting vectors are produces less, decay predominantly into gauge bosons and two-fermion final states can be extremely rare.

The results can be presented as contours in the parameter space $(g_V c_H, g^2/g_V c_F)$, as shown in fig. 1. The yellow area represents the region excluded by the 8 TeV CMS search for a 2 TeV resonance decaying into $l\nu$ [5] and the very close lying dashed yellow line depicts the $l\nu$ search at 13 TeV [6]. The two exclusion regions are almost identical since the increase in parton luminosities from 8 to 13 TeV compensates for the reduced sensitivity at 13 TeV. The dark blue region shows exclusions from the di-boson search in the two fat jet final state at 13 TeV [7]. The light blue region represents the exclusion from the 13 TeV CMS search into a fully hadronic and semi-leptonic final state [8]. Note that a second final state is included in the 13 TeV search which is why the exclusion
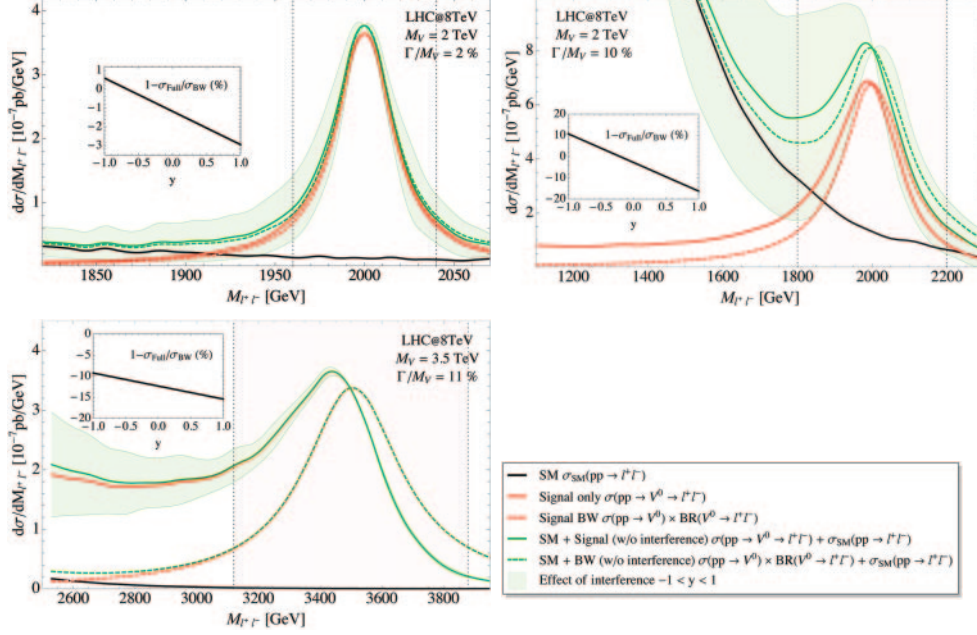
Fig. 2. – Di-lepton invariant mass distributions for a 2 and 3.5 TeV resonance.

is significantly stronger. The black contours show bounds from electroweak precision measurements, and the dashed black lines twice this value. We see that small values of $g^2/g_V c_F$ are allowed for a wide range of values for $g_V c_H$. A concrete model will simply be a point in this simplified model parameter space for a fixed value of g_V. However, this presentation makes a broad interpretation beyond specific benchmark models easy. In a very large class of explicit models of heavy vectors, the parameters c_H and c_F can be computed and the result compared with the experimental contours to asses the compatibility of the concrete model with the experimental search.

3. – Limit setting for finite widths

Experimental limits are usually set on production cross-section times branching ratio, $\sigma \times \mathrm{BR}$. This is perfectly suited to the simplified model approach since the obtained bounds are ideally completely model-independent and can be reused in any given model. In practice, setting experimental limits is not a triviality and various finite width effects have to be taken into account correctly in order to obtain truly model-independent results. These effects have been discussed in the literature [9-11] and will be reviewed in this section for the case of a heavy vector triplet. A neutral vector decaying into two leptons is the easiest example to illustrate finite width effects. In fig. 2, the di-lepton invariant mass spectrum is shown for a narrow ($\Gamma/M_V = 2\%$) and broad ($\Gamma/M_V = 10\%$) 2 TeV resonance and for a resonance of mass 3.5 TeV with $\Gamma/M_V = 11\%$ at the LHC with 8 TeV.

The first effect shows up as a significant deviation from the Breit-Wigner distribution. The dashed red lines in fig. 2 represent the Breit-Wigner invariant mass distribution normalised to $\sigma \times \mathrm{BR}$, while the red curves depict the $2 \to 2$ cross-section of the process

$pp \rightarrow V_0^* \rightarrow l^+ l^-$ obtained with MADGRAPH5. The effect is most prominent for a large mass of $3.5\,\mathrm{TeV}$ and almost absent for a narrow $2\,\mathrm{TeV}$ resonance. The effect is due to a deviation from the Breit-Wigner assumption. In order to understand this, note that the partonic cross-section of the measured signal $pp \rightarrow l^+ l^-$ is

$$(3) \qquad \hat{\sigma}_{\mathrm{S}}(\hat{s}) = \frac{4\pi\hat{s}}{3M_V^2} \frac{\Gamma_{V \rightarrow q_i q_j} \Gamma_{V \rightarrow l^+ l^-}}{(\hat{s} - M_V^2)^2 + M_V^2 \Gamma^2}.$$

The total differential cross-section can be obtained after convolution with the PDFs

$$(4) \qquad \frac{\mathrm{d}\sigma_{\mathrm{S}}}{\mathrm{d}M_{l^+l^-}^2} = \sum_{i,j} \frac{4\pi}{3} \frac{\Gamma_{V \rightarrow q_i q_j} \Gamma_{V \rightarrow l^+ l^-}}{(M_{l^+l^-}^2 - M_V^2)^2 + M_V^2 \Gamma^2} \frac{M_{l^+l^-}^2}{M_V^2} \left. \frac{\mathrm{d}L_{ij}}{\mathrm{d}\hat{s}} \right|_{\hat{s} = M_{l^+l^-}^2},$$

where $\hat{s} = M_{l^+l^-}^2$. In the peak region, the relation $M_{l^+l^-} - M_V \sim \Gamma$ holds and hence the following approximation is justified:

$$(5) \qquad \frac{M_{l^+l^-}^2}{M_V^2} \left. \frac{\mathrm{d}L_{ij}}{\mathrm{d}\hat{s}} \right|_{\hat{s} = M_{l^+l^-}^2} \simeq \left. \frac{\mathrm{d}L_{ij}}{\mathrm{d}\hat{s}} \right|_{\hat{s} = M_V^2}.$$

The differential cross-section can now be written in terms of the on-shell $\sigma \times \mathrm{BR}$, times a universal function

$$(6) \qquad \frac{\mathrm{d}\sigma_{\mathrm{S}}}{\mathrm{d}M_{l^+l^-}^2} = \sigma \times \mathrm{BR}_{V \rightarrow l^+ l^-} \mathrm{BW}(M_{l^+l^-}^2; M_V, \Gamma),$$

where BW denotes the standard relativistic BW distribution

$$(7) \qquad \mathrm{BW}(\hat{s}; M_V, \Gamma) = \frac{1}{\pi} \frac{\Gamma M_V}{(\hat{s} - M_V^2)^2 + M_V^2 \Gamma^2}.$$

The factorised result in eq. (6) only holds when the approximation in eq. (5) is valid, which might not be the case when the parton luminosities vary too strongly in the peak region. The agreement is thus stronger for smaller widths. However, even narrow resonances can be problematic at large masses. This is due to the fact that the parton luminosities decrease more rapidly at large invariant masses, which is the case at around 3 to $3.5\,\mathrm{TeV}$ for the $8\,\mathrm{TeV}$ parton luminosities. Hence the approximation is violated for larger resonance masses and the effect becomes sizeable for the $3.5\,\mathrm{TeV}$ resonance. In principle, distorted Breit-Wigner distributions could be modelled and the effect diminished. An easier alternative is to focus on the peak region only. Within the interval $[M - \Gamma, M + \Gamma]$, the areas under the dashed and solid red curves are not so different. This is quantified in the inset plots for $y = 0$. For the $3.5\,\mathrm{TeV}$ resonance the deviation is around 10%. Outside of the peak region, the deviation can be much larger, which is due to the significant tail at small invariant masses. Including this tail would set a limit on the $2 \rightarrow 2$ cross-section, instead of $\sigma \times \mathrm{BR}$.

The second finite width effect is a consequence of the quantum mechanical interference of the resonance production diagrams with the irreducible background. Of course, this depends crucially on the signal-to-background ratio and is thus less important for a heavier resonance. In fig. 2, the background is represented by the black line. The upper

and lower limit of the shaded green regions depict the result of two full simulations with constructive and destructive interference. The dashed green curve simply shows the sum of signal and SM background. This does not correspond to a realistic model since the interference does never vanish completely. We see that the effect is most pronounced for a light broad resonance. Imagining that the interference can be modelled continuously from constructive to destructive, we can write

$$(8) \qquad \frac{\mathrm{d}\sigma_{\mathrm{Full}}}{\mathrm{d}M_{l^+l^-}}(y) = \frac{\mathrm{d}\sigma_{\mathrm{B}}}{\mathrm{d}M_{l^+l^-}} + \frac{\mathrm{d}\sigma_{\mathrm{S}}}{\mathrm{d}M_{l^+l^-}} + y\,\frac{\mathrm{d}\sigma_{\mathrm{I}}}{\mathrm{d}M_{l^+l^-}}.$$

Varying y from -1 to 1 can give an idea of by how much the interference can change the shape of the distribution. Quantitative results are shown in the inset plots. Again, a reliable and simple approach is to focus on the peak region. Note that the interference vanishes exactly at $M_{l^+l^-} = M_V$ and is odd around this point. Thus the interference effect will cancel out on the two sides of the peak region, which reduces the overall effect.

We can thus conclude that staying within a narrow window around the resonance mass is crucial to obtain limits on $\sigma \times$BR. It allows us to ignore otherwise complicated finite width effects up to a certain required accuracy and to set model-independent bounds.

<div align="center">* * *</div>

REFERENCES

[1] PAPPADOPULO D., THAMM A., TORRE R. and WULZER A., *JHEP*, **09** (2014) 060.
[2] THAMM A. and TORRE R., in preparation.
[3] BARGER V., KEUNG W. and MA E., *Phys. Rev. D*, **22** (1980) 727.
[4] CONTINO R., MARZOCCA D., PAPPADOPULO D. and RATTAZZI R., *JHEP*, **10** (2011) 081.
[5] CMS COLLABORATION, *Phys. Rev. D*, **91** (2015) 092005.
[6] CMS COLLABORATION, CMS-PAS-EXO-15-006.
[7] CMS COLLABORATION, *JHEP*, **08** (2014) 173.
[8] CMS COLLABORATION, CMS PAS EXO-15-002.
[9] ACCOMANDO E., BECCIOLINI D., BELYAEV A., MORETTI S. and SHEPHERD-THEMISTOCLEOUS C., *JHEP*, **10** (2013) 153.
[10] ACCOMANDO E., BECCIOLINI D., DE CURTIS S., DOMINICI D., FEDELI L. and SHEPHERD-THEMISTOCLEOUS C., *Phys. Rev. D*, **85** (2012) 115017.
[11] CHOUDHURY D., GODBOLE R. and SAHA P., *JHEP*, **01** (2012) 155.